Size scaling for dry snow slab release

D. M. McClung
Department of Geography, University of British Columbia, Vancouver, British Columbia, Canada

Received 7 November 2002; revised 12 March 2003; accepted 2 April 2003; published 9 October 2003.

[1] Sandpile avalanches were used first to illustrate the concept of self-organized criticality (SOC). Snow avalanches consist of two types: (1) loose snow avalanches which release in cohesionless material at the top of the snowpack and (2) slab avalanches which release by propagation of shear fractures originating in a thin weak layer at depth in the snowpack. Loose snow avalanches are analogous to sandpile avalanches with a similar release mechanism, whereas slab avalanches have an entirely different release mechanism, namely, propagation of mode II shear fractures. This paper is concerned with scaling the magnitude (or size) for dry snow slabs. The argument is made that the fundamental parameter for scaling is the slab thickness based on fracture mechanics principles. The probability density function implied for the fundamental size parameter is derived from field measurements of slab thickness. An asymptotic power law is related empirically to slab fracture toughness derived from field measurements and fracture mechanical scaling. The results suggest that the power law is inversely proportional to the fracture toughness squared or, equivalently, it is inversely proportional the product of the energy to generate a unit area of fracture surface in the weak layer and the effective modulus at the base of the slab. The combined results suggest that the scaled power law is mainly explained by two components of the slab fracture toughness: (1) the fracture mechanical size effect and (2) increase in toughness due to creep, bonding, and normal pressure induced by the slab on top of the weak layer. Both components are needed to explain why fracture toughness increases with slab thickness. A further result is that release of individual slab avalanches involves a well-defined length scale which governs size and scale invariance is not satisfied. Thus slab avalanches do not conform to the original description of self-organized criticality. *INDEX TERMS:* 1827 Hydrology: Glaciology (1863); 3250 Mathematical Geophysics: Fractals and multifractals; 5104 Physical Properties of Rocks: Fracture and flow; *KEYWORDS:* avalanche, snow slab, self-organized criticality, fracture toughness

Citation: McClung, D. M., Size scaling for dry snow slab release, *J. Geophys. Res.*, *108*(B10), 2465, doi:10.1029/2002JB002298, 2003.

1. Introduction

[2] The concept of self-organized criticality (SOC) was introduced by *Bak et al.* [1987, 1988] and explained in the popular book by *Bak* [1996]. The prototype for demonstration of SOC was sandpile avalanches failing in essentially cohesionless sand. Later [e.g., *Jensen*, 1998], it was found that sandpile avalanches have a length scale associated with their release and inertial effects prevent them from obeying SOC as originally defined by *Bak et al.* [1987, 1988]. Essentially, inertial effects prevent access to a large number of metastable states in the final flow configurations so that avalanches of any size are not possible. Such avalanches are analogous to loose snow avalanches failing in near surface cohesionless snow [e.g., *McClung and Schaerer*, 1993]. Loose snow avalanches are of limited practical importance since they are usually small without large destructive effects.

0148-0227/03/2002JB002298$09.00

[3] Slab avalanches, however, usually consist of large masses of snow characterized by high speeds and with great destructive potential. They release by initiation of a propagating shear fracture in a weak layer below a cohesive slab [*McClung*, 1979, 1981, 1987, 1996; *Bažant et al.*, 2003]. It has been shown by *Bažant et al.* [2003] that the fundamental scaling parameter for release of the snow slab is the slab thickness from the perspective of fracture mechanics. This suggestion provides the fundamental starting point for discussion of scaling and self-organized criticality in this paper.

[4] Complete demonstration of self-organized criticality as defined by *Bak et al.* [1987, 1988] consists of three parts: (1) the phenomenon must exhibit critical behavior; (2) there is no intrinsic size effect (meaning that the same mechanism applies regardless of ''size'' and a log-log plot of exceedance probability versus size is essentially linear over several orders of magnitude for the fundamental dimension of size chosen to represent the phenomenon; this aspect is called self-similar spatial criticality by Bak et al.); and (3) time arrivals of events, when looked at in the frequency domain,

have a power spectrum which falls off with a negative power of frequency analogous to "flicker noise." Here, only the first two of these criteria are analyzed.

[5] In this paper, field measurements from 696 slab avalanches are used to analyze size scaling for the snow slab. The results show that the probability density function for the fundamental scaling parameter D (the slab thickness) follows a lognormal distribution from which the frequency power spectrum for thickness scaling is derived. From the data, it is shown that a log-log plot of exceedance probability versus D is nonlinear (curved) rather than linear so that scale invariance is not satisfied over any significant range of D. However, a linearized asymptotic approximation to the curved relationship is shown to be inversely proportional to a similar relationship for the slab fracture toughness squared when scaled with D.

[6] The results of this paper are that (1) there is a fundamental length scale, D, associated with dry slab avalanche release (this suggests that SOC as originally defined by *Bak et al.* [1987, 1988] does not apply to the snow slab) and (2) the linearized power of the size scaling law based on a log-log plot of exceedance probability versus D appears to be explainable by the fundamental fracture release mechanism (the implication is that the noninteger power is related to two effects on fracture toughness [*Bažant et al.*, 2003]: first, the fracture mechanical size effect law and, second, the effects of increasing fracture toughness induced by creep and bonding processes in combination with the overburden weight of the slab over the weak layer. These two effects may be summarized to describe the magnitude-frequency plot based on slab thickness: large avalanches are rarer than small avalanches due to increases of fracture toughness by both effects.

2. Self-Organized Criticality for the Snow Slab: Critical State Phenomenon and Size Parameter *D*

[7] Earlier work suggests that the release mechanism of slab avalanches is by self-propagating shear fractures in a weak layer beneath a cohesive snow slab [*McClung*, 1979, 1981, 1987, 1996]. Alpine snow fails in the weak layer by a strain-softening process [*McClung*, 1977] induced by applied load after a critical length is reached to satisfy the energy criterion for self-propagation. Thus alpine snow is a quasi-brittle pressure sensitive material subject to fracture mechanical size effects [*Bažant et al.*, 2003]. The snow slab reaches an unstable state when the applied load interacts with macroscopic imperfections in the weak layer which concentrate deformation and stresses. The initiation process normally occurs by application of load at the top of the snowpack in combination with deformation in the weak layer to yield rapid fracture [*McClung*, 1979, 1981, 1987].

[8] Typically, snow slabs result from slow application of load by wind or new snowfall (the most common cause), or from humans (skier or snow mobile or application of explosives). In common with some systems which evolve into SOC [e.g., *Jensen*, 1998] there is a transition in timescales: the processes associated with avalanche formation and the external driving of the system (most commonly storm loading) are much slower than the internal relaxation process (dynamic, mode II fracture propagation in the weak layer). The result is a planar block of cohesive snow cut out by fractures (snow slab) which is normally limited in depth down to the weak layer: D. Occasionally, an initial slab with a thickness, D, releases on a weak layer and the downslope slab dynamic movement causes the fracture to step down to a deeper, older weak layer but such cases are uncommon and they do not represent the fundamental process. Thus the fundamental length scale associated with most avalanche initiation is the depth of the snow slab D down to the weak layer which has fractured.

[9] Field observations and measurements suggest the following points:

[10] 1. Dry snow slabs move into an unstable state followed by a rapidly propagating shear fracture in a weak layer after which a catastrophic event follows.

[11] 2. There is an important length scale: the slab thickness, D, above the weak layer which governs the size of individual snow slabs. Field measurements after fallen slabs show that other estimates (e.g., crown length, slab width, and length) can increase with D but, from the perspective of the fundamental release mechanism, D governs the size. *Jensen* [1998] argues that for SOC to apply as defined by *Bak et al.* [1987, 1988] a large number of metastable states must be attainable once the threshold for criticality is achieved so that avalanches of any size are possible. This prescription clearly does not apply to dry snow slab release. Field observations and measurements show that when slab avalanches occur in a region in a short period of time (e.g., duration of a storm) they are nearly all of the same size since the size is limited to D (depth to the weak layer).

[12] 3. Slab avalanches in nature can occur with a variety of sizes over the course of a winter or over a large enough spatial (e.g., regional) scale. The physical appearance and stratigraphy of dry snow slabs suggests that they have similar characteristics regardless of size: the slab is planar with a fracture line perpendicular to the bed surface over which they release [*Perla*, 1971; *McClung*, 1981] and this physical appearance suggests that they might form a self-similar (scale invariant) set of objects. However, an analysis (presented below) shows that scale invariance is not satisfied over any significant range of D. Thus, although slab avalanches may appear to form a geometrical, self-similar set of objects, mathematically they do not follow scale invariance.

3. Fracture Mechanical Size Effects for Triggering Dry Slab Avalanches

[13] Alpine snow is a pressure-dependent, dilatant strain-softening material with significant temperature and rate dependence when failed in shear [*McClung*, 1987]. Since it is a strain-softening material it is classed as quasi-brittle and, as a result, there will be a fracture mechanical size effect which governs fracture initiation. Thus the failure cannot be described in terms of plasticity [*Bažant and Planas*, 1998] but fracture mechanics must be used. If plasticity governed, the mechanical failure criterion could be developed in terms of stress and strain and their invariants, i.e., geometrically small and large snow slabs would fail at the same maximum stress, or at the same nominal shear stress (the average shear stress applied to a cross section of the slab) with no size effect dependence contained in the failure criterion.

[14] According to *Bažant and Planas* [1998], there are two size effects related to failures of strain-softening materials which call for use of fracture mechanics. One of these is related to the deformation at which structures (slab avalanches in this case) become unstable under a given type of loading. Larger structures (avalanches) are predicted to become unstable closer to the peak on the softening curve in the failure process with smaller ones becoming unstable further into the softening range. The amount of softening prior to fracture in lab tests is also related to the type of loading (e.g., strain or load controlled) applied. However, the catastrophic failure of a snow slab must always be close to the load controlled condition for which the instability condition is reached when applied loads approach peak strength [*Bažant et al.*, 2003].

[15] The second type of size effect from fracture mechanics is related to increasing fracture toughness as the size (for example the value of D for the slab avalanche) increases. This second size effect is the fundamental one for discussion of scaling for the snow slab since it involves D: the fundamental size parameter for the fracture release process.

[16] The necessity of size effects on natural failures involving strain-softening materials was recognized by *Palmer and Rice* [1973], and they illustrated the concept for landslides in overconsolidated clay. Using nonlinear fracture mechanics they showed that there is a finite size associated with the fracture process zone, $2cf$, for which strain softening is taking place (shear stress drops from peak to residual) and they derived relationships for the mode II fracture energy required to form a crack of unit area. The formalism of Palmer and Rice was applied to the snow slab by *McClung* [1979, 1981, 1987] following the discovery [*McClung*, 1977] that alpine snow fails as a dilatant, strain-softening material in simple shear.

[17] *McClung* [1979], *McClung and Schweizer* [1999], and *Schweizer* [1998] have given estimates of cf derived from strain-softening shear failure experiments on alpine snow. The estimates of c_f (comparable to typical snow slab thickness) for alpine snow are consistent with the results estimated for concrete by *Bažant and Planas* [1998]. For concrete, *Bažant and Planas* [1998, p. 111] showed that the minimum size for analyzing the size effect associated with the length scale D is on the order of 100 times the maximum aggregate size. The typical grain size in snow is on the order of 1 mm, so the minimum size for D is expected on the order of 0.1 m: a size generally too large for laboratory shear tests. *Kirchner et al.* [2002a, 2002b] performed tensile tests on snow beams 0.2 m thick and they found that critical crack lengths were on the order of 0.1 m. In order to study variations due to the size effect, specimens would have to extend to an order of magnitude larger.

4. Fracture Mechanical Size Effect Law Containing *D* for the Dry Snow Slab From Nonlinear Fracture Mechanics With Finite Residual Stress

[18] Assuming dry slab avalanches initiate by propagating mode II shear fractures, it is important to investigate slab fracture toughness. *Kirchner et al.* [2002a, 2002b] and *Faillettaz et al.* [2002a] investigated fracture toughness for small homogenous samples of snow. Here, however, the emphasis is on slab fracture toughness for which fracture mechanical size effects and other mechanical properties are crucial.

[19] *Bažant et al.* [2003] developed the theory for the dry snow slab assuming quasi-brittle (strain-softening) behavior in the weak layer with a finite sized fracture process zone and finite residual shear stress downslope from the fracture process zone. The finite fracture process zone with strain softening is what makes the brittle, classical theory of elastic brittle fracture as developed by *Griffith* [1921, 1924] inapplicable to the snow slab. The theory here takes the assumption of elastic slab behavior when it is failing with strain-softening behavior taking place in a finite region of the weak layer beneath the slab. See *Bažant et al.* [2003] for additional assumptions and qualifiers on the theory which include: ignoring viscoelastic effects and the assumption that the snowpack material below the weak layer has a much higher modulus than the slab.

[20] From *Bažant et al.* [2003] the expression for the stress intensity factor, K_{II}, for mode II loading in terms of nominal shear stress at failure, τ_N for large sizes (relative to the fracture process zone) is given by

$$K_{\mathrm{II}} = \tau_N(1 - \tau_r/\tau_N)\left(\alpha_0\sqrt{D/2}\right) = \sqrt{E'G_{\mathrm{II}}} \qquad (1)$$

where α_0 is a material constant of order 1, G_{II} is fracture energy of snow to create a unit area of sliding crack, τ_r is residual stress and the expression is written for $D \gg c_f$ (where $2cf$ is length of the fracture process zone). In equation (1), E' is the effective Young's modulus at the base of the snow slab. The nominal applied shear stress for a planar snow slab on a slope of constant angle (Ψ) is estimated as $\tau_N = \rho g\, D \sin\Psi$, where g is the magnitude of acceleration due to gravity, ρ is mean slab density, and Ψ is slope angle. Figure 1 is a schematic showing slab geometry and the lengths: D and $2cf$. If avalanches are triggered by processes involving dynamic loads (e.g., skiers or explosive control), then equation (1) needs modification. This is discussed in a later section.

[21] Following *Bažant et al.* [2003] with either the assumption that τ_r/τ_N is small relative to 1 or that the τ_r and τ_N are proportional to the same power of D (as might be approximately expected for a pressure-dependent material like alpine snow), the mode II fracture toughness may be approximated by equating shear stresses to shear strengths and K_{II} to $K_{\mathrm{II}c}$ (fracture toughness):

$$K_{\mathrm{II}c} = \sqrt{E'G_{\mathrm{II}}} \propto \tau_N\alpha_0\sqrt{D/2}, \qquad D \gg c_f. \qquad (2)$$

Thus, for large sizes, fracture toughness scales approximately as $K_{\mathrm{II}c} \propto \tau_{\mathrm{N}}D^{1/2}$. In (2), there are two important effects: the dependence of τ_{N} on D (shown below to depend on creep, normal pressure and bonding effects under the slab overburden) and the square root dependence derived from nonlinear fracture mechanics. Both of these effects must be considered in order to explain the mode II fracture toughness of the snow slab which is central to snow slab release.

5. Dependence of Nominal Shear Strength Scaled From Field Measurements at Fracture Lines

[22] The fracture mechanical size effect of *Bažant et al.* [2003] is derived from the assumption that the failing material is the same underneath the snow slab at all sizes.

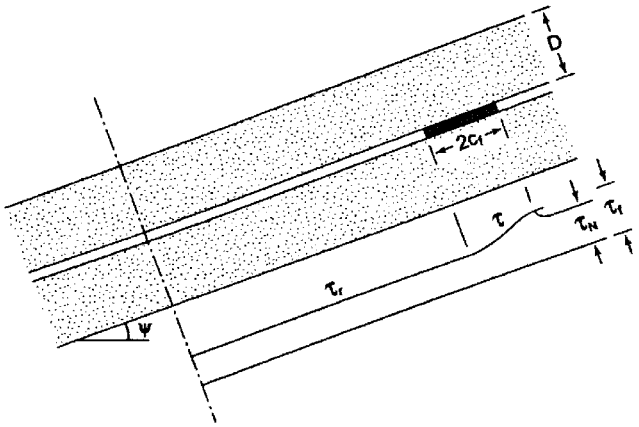

Figure 1. Schematic of slab and weak layer with fundamental size effect parameter D. Strain softening occurs in the weak layer subject to nominal applied shear stress τ_N, peak shear strength τ_f, and residual strength τ_r.

This condition will not be satisfied for slab data collected on mountain slopes since snow and mechanical properties will vary from place to place. For example, the weight of the snow above the weak layer and the age of snow at the weak layer have major effects on the properties of snow at the base of the snow slab. An increase in thickness, which is often accompanied by increased age of snow at the base, will cause densification and bonding to increase the Young's modulus and enhanced bonding will increase the nominal shear strength. The combined effects of creep, bonding and normal pressure effects under load must be taken into account in order to adequately describe fracture toughness for a collection of data taken in the field. These effects combine to vary the fracture toughness in addition to the fracture law size effect. For the data here, it would not be correct to attribute these effects directly to shear strength since the concept of shear strength cannot be isolated in snow slab release which is governed by fracture and strain softening [*Bažant et al.*, 2003]. Instead, shear strength is contained within slab fracture toughness which depends on many variables.

5.1. Field Data From Fallen Snow Slabs

[23] I have collected data taken from the 187 fracture lines of dry fallen snow slabs. The data contain field measurements of mean slab density, the average slope angle that the slabs have initiated on and the average depth D of the slabs at the fracture line. The sources of the data include *Perla* [1976], *Stethem and Perla* [1980], and data from the collection of the J. Schweizer, Swiss Federal Institute for Snow and Avalanche Research. The data include avalanches with a mix of triggers including mostly natural triggers such as snowfall or loading from blowing snow, skier triggering and explosives (the triggering aspect is discussed below). Figure 2 depicts a least squares regression line for τ_N as a function of D. The equation of the least squares line is

$$\tau_N = CD^{1.22}. \tag{3}$$

In equation (3), 82% variance of τ_N with D is explained (R^2 = 0.82, where R is Pearson cor1relation coefficient, standard error is 0.33 for 187 values). The value of C is 1.36 kPa/m$^{1.22}$. The 95% confidence limits on the power of D are between 1.13 and 1.30.

5.2. Fracture Toughness Scaling Law

[24] Combination of equations (3) and (2) gives a scaling law for the fracture toughness from the fracture scaling size effect law and the material effects of creep, bonding, normal pressure and crystal forms on τ_N [*Bažant et al.*, 2003]:

$$K_{IIc} = \sqrt{E'G_{II}} \approx \left(\alpha_0 C/\sqrt{2}\right) D^{1.72}. \tag{4}$$

Equation (4) implies that $K_{IIc}^2 = E'G_{II} \propto D^{3.44}$. Thus K_{IIc}^2 has a noninteger power of $D \approx 3.44$ and it is related to the product of the energy for mode II fracture energy of snow, i.e., the energy required to form a unit area of sliding crack and the effective modulus E' at the base of the slab.

[25] For slabs with $D \geq 0.50$ m, equation (4) is replaced by

$$K_{IIc} = \sqrt{E'G_{II}} \approx \left(\alpha_0 C/\sqrt{2}\right) D^{1.78}, \tag{5}$$

which implies $K_{IIc}^2 = E'G_{II} \propto D^{3.56}$. Equation (5) results from a least squares analysis yielding: $\tau = 1.37\ D^{1.28}$ with R^2 = 0.70, standard error 0.31 for 118 dry slabs. For this analysis, 95% confidence limits on the power of D from calculations of τ_N are 1.13–1.44.

[26] *Mellor* [1975] presents data on the density dependence of the Young's modulus of snow. The data show that in the density range 100–300 kg/m^{3,} which is applicable for most slab avalanches [*McClung and Schaerer*, 1993], the Young's modulus increases by about a factor of 100. In the alpine snowpack, the densification will arise from time and temperature-dependent creep under the snow slab overbur-

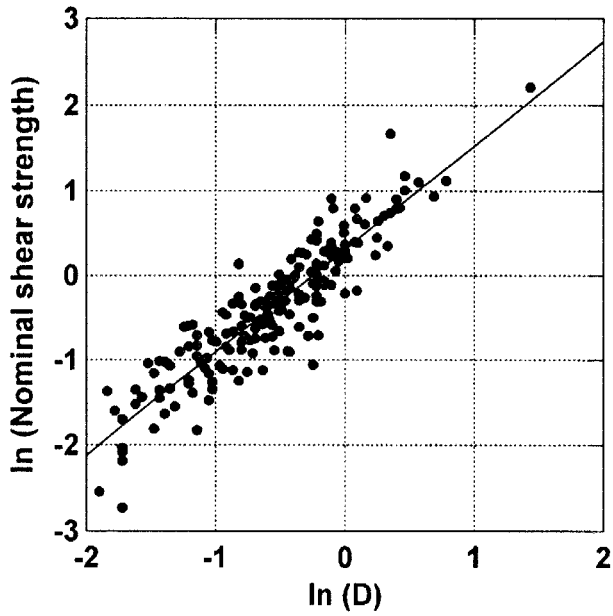

Figure 2. Plot of ln(τ_N) versus ln(D) from field measurements at fracture lines of fallen dry snow slabs.

den prior to the fracture process. Density and, therefore, Young's modulus G_{II}, and, consequently, fracture toughness may also affected by wind packing during deposition.

[27] For the cohesive crack model with strain softening in the fracture process zone [e.g., *Palmer and Rice*, 1973], G_{II} has an interpretation as the area under the softening curve as the material softens from peak, τ_f, to residual, τ_r, given by: $(\tau_f - \tau_r)w_f$, where w_f (approximately a material constant) is the mean displacement. From laboratory data on shear failures, both the peak and residual strengths are dependent on normal pressure. Therefore, on the basis of these properties of snow, it is expected that K_{IIc}^2 should be dependent on creep and pressure dependence at the base of the slab as in equation (5).

[28] Equation (4) suggests that K_{IIc} increases by a factor of about 50 as D increases from 0.25 to 2.5 m. For such values of D, mean slab snow density should range from about 100 (0.25 m slab) to 300 kg/m^3 (2.5 m slab) with E' increasing by about 2 orders of magnitude [*Mellor*, 1975, p. 258] and peak shear strength [*McClung and Schaerer*, 1993, p.71] increasing roughly by about a factor of 50. The product E′ and τ_f as related to G_{II} from the cohesive crack model suggest in a very rough sense that K_{IIc} for the snow slab could increase by about a factor of 70 (ignoring residual strength as with the fracture toughness scaling law) as density increases from 100 to 300 kg/m^3 in rough agreement with predictions of the scaling law (4).

[29] Given that α_0 is of order 1 [*Bažant et al.*, 2003], equation (4) suggests values of slab fracture toughness could be in the approximate range 0.1–5 kPa(m)$^{1/2}$. The values compare with snow fracture toughness estimates from small samples on order of 1 kPa(m)$^{1/2}$ [*Kircher et al.*, 2002a, 2002b]. The values for slab toughness and snow may be compared to values for concrete and steel [*Bažant and Planas*, 1998] of 10^3 kPa(m)$^{1/2}$ and 10^5 kPa(m)$^{1/2}$, respectively. The extremely low fracture toughness for the snow slab provides a partial explanation for the high frequency of slab avalanches compared to landslides and other types of slope failures which have higher shear strength and effective Young's modulus than alpine snow.

6. Effect of Failure Layer Temperature

[30] The properties of snow are sometimes temperature-dependent which could influence the results in this paper. For example, creep and bonding processes are highly temperature-dependent. However, *McClung* [1996] showed, on the basis of the results of *Sinha* [1981, 1984] that, for elastic deformation, alpine show is expected to be nearly temperature-independent: the elastic Young's modulus of the matrix material (ice) is nearly temperature-independent over a wide range of temperatures.

[31] Figure 3 depicts failure layer temperatures for 123 dry slab avalanches. The data show a very narrow range of temperatures: all within essentially 5% of the melting point on the Kelvin scale. The mean of the data scaled relative to the melt temperature (273.16°K) is 0.98 with a standard deviation 0.01.

[32] The narrow range for the temperature data coupled with the expectation that the elastic Young's modulus is nearly temperature-independent suggests that, for the present data set, the effects of temperature should be small or negligible with respect to the Young's modulus. *Schweizer* [1998] and *McClung* [1996] reported shear experiments in rate ranges when viscoelastic effects enter. The tangent modulus (analogous and related to the elastic Young's modulus) approximately doubles between −5°C and −15°C. Such viscoelastic effects may enter in describing slow crack initiation and growth but once fracture initiates the deformation rates will be rapid and a purely elastic (temperature-independent) model is more suitable since snow is essentially elastic at high deformation rates.

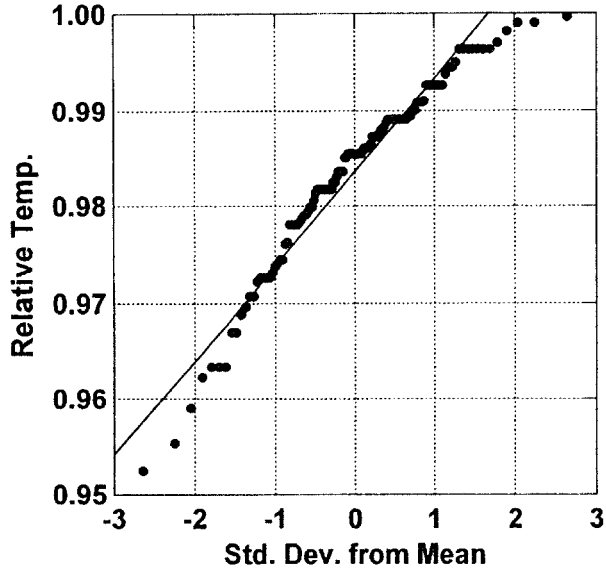

Figure 3. Probability plot of failure layer temperature relative to the melt point (273.16°K). Mean is 0.98, and standard deviation is 0.01. The least squares line represents a normal distribution.

[33] A multiple regression for τ_N as a function of D and the relative temperature (123 cases): T(°K)/(273.16°K) showed that temperature is not significant. The failure strength (peak in a strain-softening experiment) is nearly temperature-independent [*McClung*, 1996; *Schweizer*, 1998] so this result is not surprising. For the present data set, therefore, it may be concluded that the effects of the failure temperature at time of slab initiation at the base of the slabs are small or negligible. The data collection is expected to be representative of slab avalanches in nature (most failure temperatures above −15°C) so there is some support for the suggestion of *Bažant et al.* [2003] that the effects of temperature may be small for the fracture process.

[34] The most important effects of snow temperatures, on the basis of the analysis in this paper, seem to be associated with the highly temperature- and time-dependent creep and bonding processes [*McClung*, 1996]. Thus it is expected that slab fracture toughness is temperature- and time-dependent with toughness increasing both with time and temperature due to the related processes of creep and bonding. This effect is often noted by avalanche forecasters: newly fallen snow at high temperatures is subject to rapid bonding and densification under the slab overburden so that period of instability passes more quickly than for colder snow. Both

creep and bonding will also depend importantly on the overburden (slab depth) at the weak layer.

7. Weak Layer Anisotropy Aspect of Fracture Toughness

[35] Some weak layer crystal forms such as surface hoar, facetted snow and depth hoar appear to be anisotropic in their mechanical behavior [*McClung and Schweizer*, 1999] since they resist creep (densification) under a slab overburden. Instead, they can be extremely prone to slope-parallel shear deformation. Such anisotropy is expected to be an important aspect of fracture toughness. Field observations show that surface hoar and facetted snow in weak layers are extremely prone to producing shear fractures leading to slab avalanche release. *Jamieson* [1995] calls weak layers with such crystal forms "persistent weak layers" since they can persist for long periods in the snowpack resisting densification and bonding under the slab overburden. The propensity of such anisotropic forms to resist bonding/densification and to form shear fractures is expected to be an important practical aspect of slab fracture toughness but quantification is beyond the scope of the present paper.

8. Power Law Scaled From Measurements of *D*

[36] Since slab avalanches have a physical appearance that is similar regardless of size D, it is appropriate to investigate whether scale invariance applies over any significant range of D. If so, slab avalanches might constitute a self-similar set of objects as defined for SOC by *Bak et al.* [1987, 1988].

[37] It is shown below that to a very good approximation D follows a lognormal probability density function or equivalently $\ln(D)$ follows a normal distribution. The probability density function is fundamentally related to the frequency power spectrum below.

8.1. Power Spectrum of ln(*D*)

[38] Figure 4 represents a probability plot of $\ln(D)$ which shows that the probability density function of $\ln(D)$ is Gaussian to a good approximation. For brevity, let $x = \ln(D)$. With the inverse Fourier transform, the probability density function, $p(x)$, may be obtained from the characteristic function $\varphi(\omega)$, where ω is angular frequency:

$$p(x) = \frac{1}{2\pi} \int_{-\infty}^{\infty} \phi(\omega) e^{-i\omega x} d\omega \tag{6}$$

From equation (6), the power spectral density, $S_X(\omega)$ is then defined as

$$S_x(\omega) = \frac{1}{2\pi} \phi(\omega) \phi * (\omega) \tag{7}$$

where $\varphi^*(\omega)$ is the complex conjugate of $\phi(\omega)$.

[39] From Figure 4, $p(x)$ is given by

$$p(x) = \frac{1}{\sigma\sqrt{2\pi}} \exp\left[-(x-\mu)^2/2\sigma^2\right], \tag{8}$$

where μ is the mean of x and σ is the standard deviation.

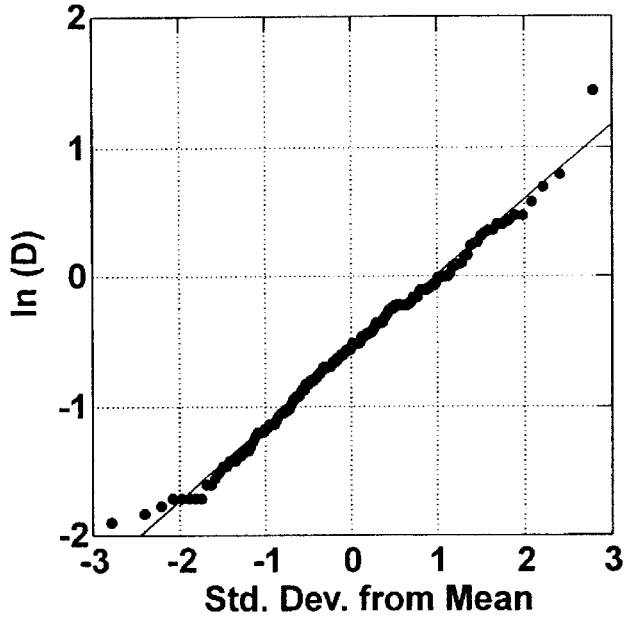

Figure 4. Probability plot for $\ln(D)$ for 187 dry slabs with a mix of triggers. The least squares line shows the fit to a normal distribution. The plot suggests that $\ln(D)$ obeys a normal distribution. The abscissa represents standard deviations of $\ln(D)$ from the mean.

[40] Integration gives the power density spectrum of $\ln(D)$:

$$S_X(\omega) = 1/2\pi \exp\left(-\sigma^2\omega^2\right). \tag{9}$$

Equation (9) shows that the power spectrum for $\ln(D)$ falls off exponentially with ω^2 and it illustrates that the probability density function is fundamentally related to the frequency power spectrum. For 187 dry slabs, the value of σ in equation (9) from sample statistics is 0.58. Note that S_X does not constitute a constant power spectrum. It can easily be shown that if $p(x)$ in equation (8) was replaced by a Dirac delta function, a constant power spectrum $S_X(\omega) = 1/2\pi$ would result implying "white noise" which is incompatible with the concept of self-similar criticality as defined by *Bak et al.* [1988]: the power spectrum must fall off as the frequency increases for self-similar criticality so that most of the "power" is contained in the low frequency (large) events. For equation (9), the contribution to the power spectrum for $\omega > 4\pi$ is negligible.

8.2. Power Spectrum of *D*

[41] Since D is the fundamental scaling parameter for the snow slab, it is required to investigate the power spectrum of D instead of $\ln(D)$. Figure 4 shows that D obeys a lognormal probability density function to a good approximation. Therefore $p(D)$ may be represented as

$$\begin{aligned} p(D) &= \frac{1}{D\sigma\sqrt{2\pi}} \exp\left\{-[\ln(D)-\mu]^2/2\sigma^2\right\}, \qquad D \geq 0 \\ p(D) &= 0, \qquad\qquad\qquad\qquad\qquad\qquad\quad D < 0 \end{aligned} \tag{10}$$

where μ is the mean of $\ln(D)$ and σ is the standard deviation of $\ln(D)$. The power spectrum is defined by equation (6)

(with D replacing x) and equation (7). The integration implied by equation (7) yields a series with infinitely many terms. Expansion of the first three terms yields the character of the power spectrum:

$$S_D(\omega) = \frac{1}{2\pi}\left[I_1^2 - \omega^2\left(I_1 I_3 - I_2^2\right) + \omega^4\left(I_5 I_1/12 + I_3^2/4 - I_2 I_4/3\right)\ldots\right]. \quad (11)$$

In equation (11), the terms with I subscripted represent the results of integrals with values given by

$$I_n = \exp\left\{(n-1)\left[\mu + \left((n-1)\left(\sigma^2/2\right)\right)\right]\right\}, \quad (12)$$

where n takes integer values 1–5.

[42] As with equation (9), equation (11) shows how the power spectrum falls off with ω. For numerical evaluation in (12), $\mu = -0.57$ and $\sigma = 0.58$ estimated from sample statistics. Again, most of the power is contained in the low frequency (high values of D) as is implied for self-similar criticality as a component of SOC.

9. Asymptotic Expression for pdf of *D* for Large Values of *D*

[43] The analysis above shows that the pdf of D is fundamental since the power spectrum is derived from it. In order to compare the power law implied by the fracture mechanics scaling with an approximate relationship implied by the pdf, it is necessary to explore a log-log probability plot versus D for the "low frequency" (large events). Figure 5 shows a plot of nonexceedance probability versus D for the data set using rank order statistics and Hazen plotting positions. Figure 6 is a log-log plot for the portion of the data for which $D \geq 0.50$ m. The least squares line fitted through the data for values of $D \geq 0.50$ m gives a (negative) power of -2.60 with 95% confidence limits between -2.52 and -2.69, $R^2 = 0.97$ with a standard error of 0.18.

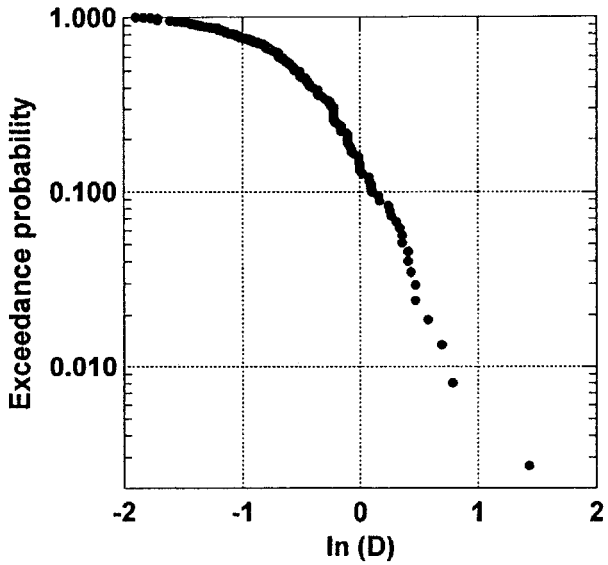

Figure 5. Log-log plot, ln(exceedance probability) versus ln(D) for 187 dry slabs with a mix of triggers.

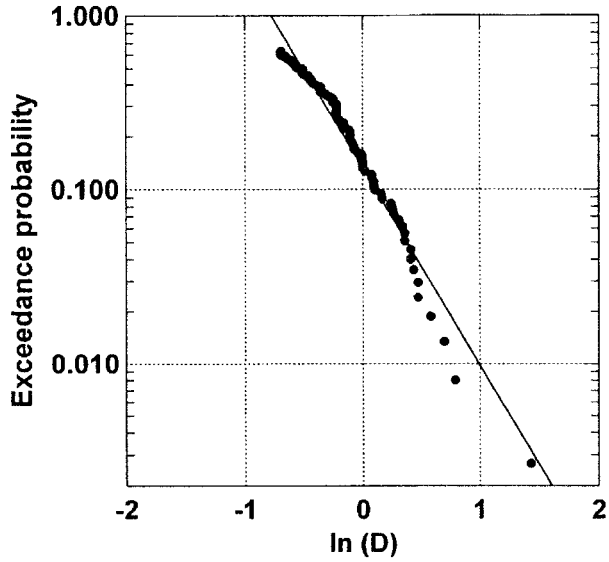

Figure 6. Asymptotic exceedance probability for slabs with $D \geq 0.50$ m. The least squares line has a slope of -2.60. Percent variance explained is 97% ($R^2 = 0.97$).

[44] Figure 6 is the classical representation normally used to discuss self-similar criticality: a straight line with negative slope on a log-log plot of exceedance probability versus the characteristic size (D in this case). However, the data plotted in Figure 4 suggest that the plot in Figure 6 is a curved relationship represented by the lognormal pdf for D. Since the log-log plot is not linear, it suggests that scale invariance (fractal behavior) does not apply to the present data set over any significant range of values. This result, combined with the previous discussion of an important length scale, suggests that at least two criteria for SOC as defined by *Bak et al.* [1987, 1988] are not satisfied for the snow slab. SOC is supposed to involve scale-invariant behavior and lack of a length scale but neither applies to the snow slab.

[45] The entire power spectrum implied for the pdf is more fundamental than the plot in Figure 6 which represents a censored, linearized plot. However, the analysis implied by Figure 6 is convenient to compare with the asymptotic power derived from the fracture mechanical scaling (equation (5) and following).

10. Fracture Mechanical Explanation of Size Scaling

[46] The analysis in Figure 6 implies that the exceedance probability, $P(\geq D)$ falls off with the power on the asymptote ($D \geq 0.50$ m):

$$P(\geq D) \propto 0.11 D^{-2.60}. \quad (13)$$

The relation implies that the cumulative distribution function for D is given by

$$P(\leq D) = 1 - 0.11 C D^{-2.60} \quad (14)$$

where C is a constant. *Rosenthal and Elder* [2002] plotted slab data from more than 8000 avalanches and obtained a power law similar to (13): power $D^{-2.60}$.

[47] From equation (14), the asymptotic probability density function for D is the derivative of equation (14) with respect to D:

$$p(D) \propto 0.29\ D^{-3.60}, \quad D \geq 0.50 \text{ m} \tag{15}$$

Equation (15) implies the probability that D is between D and $D + dD$ is $p(D)dD$.

[48] The analysis below equation (5) shows for $D \geq 0.50$ m, that $K_{IIc}^2 \propto D^{3.56}$. Given the confidence limits on the powers, the implication is that the pdf of D is inversely proportional to K_{IIc}^2 which is proportional to the product of energy needed to create a unit area of crack (or fracture surface) and the effective modulus. Thus the noninteger power in equation (15) has a possible explanation in the components of fracture toughness: the fracture size effect and the effects of creep, bonding and normal pressure effects at the base of snow slabs. The answer to the question: "Why are large D slabs rarer than small ones?" seems rooted in the components of fracture toughness and the absolute value of the noninteger power in equation (15) matches that K_{IIc}^2 implied by equation (5) very closely. The rarity of larger events and the power spectrum in relation to sizes (most power in the rare, large size events, e.g., equation (11)) is fundamental to size scaling as a component of self-organized criticality according to *Bak* [1996]. Calculations of $K_{IIc}^2 \propto \tau_N^2 D$ as in equation (2) showed that K_{IIc}^2 obeys a lognormal pdf (see Figure 7) as does D (see Figure 4). A probability plot of τ_N from the data revealed that it also obeys a lognormal distribution. Since both D and τ_N follow lognormal pdfs it is expected that K_{IIc}^2 is lognormal since it is formed from the product of two lognormal variables.

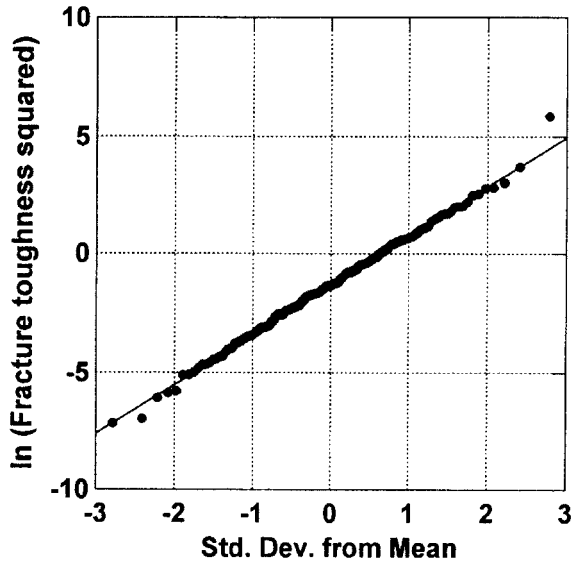

Figure 7. Lognormal probability density function for K_{IIc}^2, fracture toughness squared similar to Figure 4. The calculations are based on the product of τ_N^2 and D as from equation (2). The estimates are from 187 dry slab avalanche fracture lines with a mix of triggers.

11. Effects of Triggering Mechanism Including Skier Triggering

[49] The data in the above analysis include slab avalanches which have released by a mix of triggers including mostly natural events, some released by explosives and about 20% of the avalanches triggered by people on skis. To analyze the triggering effect, the skier triggered data were removed and the analysis was repeated. The analysis showed that the powers (e.g., equations (5) and (15)) changed slightly but the basic results obtained above were not altered. A subset of 33 skier triggered avalanches was also analyzed separately with similar results: the pdf was lognormal and the noninteger powers for the asymptotic pdf and inverse square of K_{IIc} were essentially the same.

[50] A subset of 56 natural avalanches (not triggered by humans) was also analyzed. The data showed that D followed a lognormal pdf with mean of $\ln(D) = -0.63$ and standard deviation of $\ln(D) = 0.50$. Analysis showed that the asymptotic form of the pdf (for $D \geq 0.50$ m) had a power proportional to $D^{-4.4}$ (95% confidence limits -3.9 to -4.8). Estimates of the fracture toughness scaling ($D \geq 0.50$ m) similar to equation (5) showed that K_{IIc}^2 is proportional to $D^{3.9}$ (95% confidence limits 3.0 to 4.8). This asymptotic analysis, although on the basis of limited data (35 avalanches with $D \geq 0.50$ m), provides support for the conclusion from the larger data set with a mix of triggers that the asymptotic pdf is approximately inversely proportional to K_{IIc}^2. Analysis of the full data set of 56 natural avalanches showed that both D and $K_{IIc}^2 \propto \tau_N^2 D$ obey a lognormal distribution as with the full data set of 187 avalanches with a mix of triggers (Figure 7).

[51] I also collected a data set containing values of D for 453 avalanches which were triggered by skiers. Since I do not have slab density data, I am not able to estimate the fracture toughness by scaling methods. However, the data follow a lognormal distribution (see Figure 8) with mean of $\ln(D) = -0.71$, and standard deviation of $\ln(D) = 0.54$. These values compare with -0.57 and 0.58 for the data set above with 187 avalanches with a mix of triggers. This comparison shows that the power spectra for the two data sets are of the same form and support is provided for similar behavior in relation to the triggering mechanism.

12. Finite Size Effects

[52] *Bak* [1996] and *Jensen* [1998] show that self-similar scaling or scale invariance sometimes breaks down at large sizes for critical phenomena implying a finite size effect as a physical upper limit for the system is approached. The curved relationships for the log-log plots of exceedance probability and D for the data sets in this paper suggest that finite size effects may be implied (e.g., Figures 5 and 8). Since densification and bonding can work together to increase mode II fracture toughness, there may be finite limits to the size of slab avalanches depending on the energy supplied by the triggering mechanism. It is not possible for mode II fractures to propagate in an isotropic material. Given enough time and load, alpine snow can densify to ice which implies mode II fracture is impossible. This suggests an extreme upper limit as a possible finite size

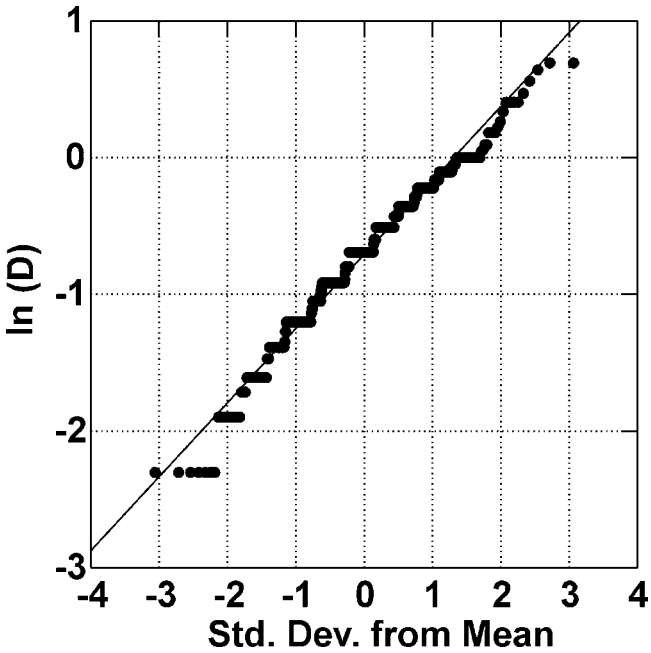

Figure 8. Probability plot for ln(D) for 453 dry slabs triggered by skiers similar to Figure 4.

effect. However, exponential increases in both Young's modulus and nominal shear strength with density should combine to increase fracture toughness producing finite upper limits to slab avalanche fracture toughness far below the theoretical ice limit.

[53] *Jensen* [1998] suggests that the existence of a finite size effect sometimes produces a cutoff in scale-invariant (fractal) power law behavior for critical systems to yield a size distribution for large sizes of the form

$$P(\geq D) - D^{-a}\exp(-D/D_0), \tag{16}$$

where a and D_0 are related constants.

[54] Nonlinear analysis for $D \geq 0.50$ m, gave excellent fits to the data sets in Figures 5 and 8. For the data with a mix of triggers (Figure 5), the result is

$$P(\geq D) = D^{-0.63}\exp(-D/0.56)$$
$$R^2 = 0.99; \quad N = 118 \text{ slabs}, \tag{17}$$

with 95% confidence limits on a, -0.66 to -0.60, and 95% confidence limits on D_0: 0.55 to 0.56.

[55] Similarly, for the skier triggered data, the analysis gave

$$P(\geq D) = D^{-0.74}\exp(-D/0.43)$$
$$R^2 = 0.97; \quad N = 266 \text{ slabs} \tag{18}$$

with 95% confidence limits on a, -0.78 to -0.70, and 95% confidence limits on D_0, 0.42 to 0.44.

[56] Figure 9 shows the odds ratio calculated from the ratio of equations (17) and (18) for D in the range of 0.5 to 2.5 m. Figure 9 shows that the odds ratio increases from about 1.2 to 4.0 for the range of D which implies that as D increases, it is increasingly rarer for skier triggered avalanches than for the data which represent a mix of triggers. *McClung and Schweizer* [1999] argued that due to limitations on deformation imparted by skiers, deep skier triggered avalanches (e.g., deeper than 1 m) are quite rare. The calculations in equations (17) and (18) support the idea of rarity of deep skier triggered avalanches and they suggest that the asymptotic form of the exceedance probability is governed by finite size effects which depend on the triggering mechanism. For example, higher energy supply, such as by explosive control or earthquake loading should produce more larger avalanches than by skier triggering and this will affect the asymptotic form of the plot of $P(\geq D)$ versus D. *Bak* [1996] suggests that finite size effects are a feature of critical systems. A feature of data from skier triggering is that the avalanches are sometimes initiated well below the crown where the slab data are taken and large ones are often triggered at thin spots so the values of D taken from the crown can be overestimates compared to the position downslope where the avalanches may have been initiated.

13. Effects of Explosive Control and Dynamic Effects

[57] The effects of explosive control compared with natural release are illustrated by the work of *Faillettaz et al.* [2002b]. They constructed separate cumulative probability plots for D for explosive controlled avalanches (sample size several thousand) and naturally released avalanches (sample size about 200). Their analysis showed that

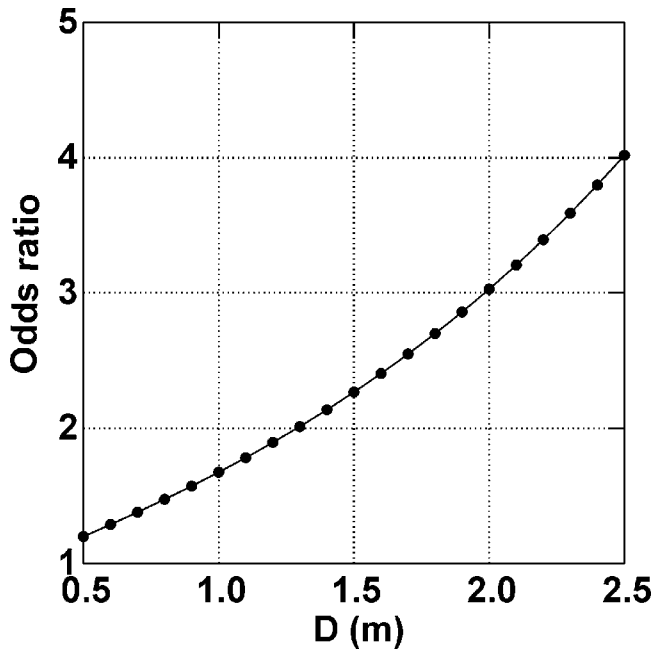

Figure 9. Odds ratio calculated for D in the range 0.5 to 2.5 m based on the ratio of $P(>D)$ for a mix of triggers (equation (17)) to that for skier triggering (equation (17)). The plot suggests that skier triggered avalanches are increasingly less likely as D increases compared to the data for a mix of triggers.

$P(\geq D)$ fell off approximately as $D^{-2.5}$ for the avalanches triggered by explosives which may be compared with equation (13) for which $P(\geq D)$ on the asymptote falls off as $D^{-2.60}$. For naturally triggered avalanches, *Faillettaz et al.* [2002b] calculated that $P(\geq D)$ fell off approximately as $D^{-2.2}$. Their data suggest that the asymptotic exponent of D is related to the triggering mechanism. The asymptotic powers calculated by *Faillettaz et al.* [2002b] can not be directly compared with those in this paper since different assumptions were used by them to plot the values and determine the cutoff value of D to define the asymptote. From the formalism in this paper, their data may suggest that slab fracture toughness can increase for explosive controlled avalanches over avalanches which released naturally without dynamic energy input. This feature is also suggested by the skier triggered data discussed above. However, supporting data to estimate slab fracture toughness are not available for their data.

[58] Any discussion of slab release following skier triggering must involve dynamic loading and viscoelastic effects [*McClung and Schweizer*, 1999]. Also, avalanches released by explosive control involve dynamic loads. Therefore application of the stress intensity factor represented by equation (1) is a very rough approximation at best. *Bolt et al.* [1975] applied dynamic earthquake loads to classical landslide stability evaluation by adding approximate "equivalent static force" loads from earthquakes to the estimated static, gravitational loads. If this simple prescription is applied to equation (1) then the nominal shear stress for the planar slab due to gravity loading would be replaced by one with an increased shear loading when dynamic effects enter. Thus the load at fracture might be higher for the skier triggered or explosive controlled avalanches (implying higher fracture toughness) than for natural avalanches as the above data sets suggest.

14. Summary and Conclusions

[59] Dry slab avalanches are assumed to initiate by mode II shear fracture in a weak layer preceded by strain softening [*McClung*, 1979, 1981]. This implies a size effect law for fracture [*Bažant et al.*, 2003] and that the fracture toughness, K_{IIc} governs slab release not the shear strength as classical analyses using plasticity predict. Field and laboratory measurements suggest that many factors [time and temperature, slab overburden (normal pressure), weak layer anisotropy, crystal forms, density, and rate effects] combine to determine fracture toughness for the snow slab. As with engineering materials [*Broek*, 1986], it does not seem possible to completely isolate any one of the contributing factors. The empirical, statistical nature of the theory presented here arises primarily from natural variations in fracture toughness for the snow slab due to combinations of the contributing factors.

[60] The classical infinite slope engineering stability index [e.g., *Roch*, 1966]: the ratio of shear strength to shear stress at a weak layer does not apply to snow slab release in general. Any yield criterion based solely on stress or strain is analogous to plasticity for which fracture size effects do not exist. *Kirchner et al.* [2002a, 2002b] determined fracture toughness of snow for small, homogeneous samples without consideration of fracture mechanical size effects and analogous to plasticity solutions. However, snow slab release, as treated in this paper, is a problem involving fracture initiation, strain-softening and size effects [*Bažant et al.*, 2003]. Therefore a relation between K_{IIc} and K_{II} is more appropriate for assessing snow slab instability than a relation between shear strength and shear stress.

[61] The analysis in this paper suggests that the a linear least squares fit to exceedance probability versus D for large sizes ($\geq$0.50 m) is consistent with inverse proportionality to K_{IIc}^2, where K_{IIc}^2 is the product of the energy to form a unit area of failure surface along the weak layer and the effective modulus at the base of the slab. The excellent agreement between the power of D on the asymptotic pdf ($D \geq 0.50$ m) and that for the inverse of the K_{IIc}^2 may be fortuitous. Given the uncertainties and approximations, I suggest that the proportionality between the asymptotic pdf and the inverse of K_{IIc}^2 is only an approximation. More data are needed to strengthen this conclusion in view of the approximations in this paper. At this point, the suggestion of proportionality is empirical, on the basis of field measurements rather than a rigorous theoretical treatment.

[62] The analysis here and that of *Bažant et al.* [2003] show that K_{IIc} has at least two major components: the fracture mechanical size effect law and the material effect due to creep, bonding and pressure sensitivity at the base of the snow slab underneath the slab overburden. Thus it seems possible to explain the asymptotic power displayed by the pdf of D in terms of the fracture toughness and its components. The theory suggests that large (D) avalanches are rare due to increased fracture toughness which is primarily the result of the fracture size effect law and densification-creep/bonding and pressure sensitivity effects at the base of the snow slab.

[63] For the present data set, the effects of snow temperature at the time of fracture initiation at the base of the snow slab appear to have negligible influence. This is expected for elastic fracture initiation and where temperatures vary over a small range (within 95% of the melt temperature). The primary effects of snow temperatures on fracture toughness appear to be related to the creep/bonding processes over time at the base of snow slabs: both processes being highly time- and temperature-dependent [*McClung*, 1996; *McClung and Schaerer*, 1993].

[64] Instead of asymptotic power law relationships derived from log-log plots of exceedance probability versus size, the pdf may be more fundamental since the frequency power spectrum is simply derived from it by Fourier transform integrals. The power spectrum determines the frequency relation for the entire distribution, not just the large (low frequency) events. Further, in this paper, it is suggested that the link to the fundamental critical mechanism, fracture, is through the pdf.

[65] The ideas presented here might apply to landslides and debris slides when failures are governed by strain softening. However, for the landslides or debris slides the fundamental scaling parameter D [*Bažant et al.*, 2003] is rarely measured and fracture toughness properties needed are not normally be estimated. Application of the fracture mechanics size effect law and assuming that τ_N is proportional to D (neglecting the creep, bonding and pressure sensitivity effects suggested for snow), suggests that the pdf

for planar landslide failures caused by strain softening should fall off approximately as: D^{-3} or that the cumulative distribution function of D should fall off approximately as D^{-2}. *Hovius et al.* [1997] attacked scaling for the landslide problem, but they did not provide estimates of D. Under the assumption used by *Hovius et al.* [1997] that landslide thickness is proportional to width, their data suggest an asymptotic pdf $\propto D^{-3.32}$ which is comparable to the results for snow avalanches in this paper.

[66] The analysis in this paper combined with field observations suggests that the snow slab does not obey SOC as originally defined by *Bak et al.* [1987, 1988]. The reasons are as follows:

[67] 1. There is a fundamental length scale D associated with slab release which constrains the distribution of sizes to a narrow range under a given external perturbation. A large number of metastable states associated with a large number of possible sizes are deemed necessary for SOC and this does not coincide with field observations and measurements about the snow slab.

[68] 2. The distribution of sizes for the data sets in this paper is not scale invariant or fractal over any significant range of D. The analysis suggests instead that D obeys a lognormal pdf and that finite size effects (depending on the triggering mechanism or energy supply prior to release) may produce a curved rather than a scale-invariant or fractal relationship on a log-log plot of exceedance probability versus D. Field observations and data from fallen dry snow slabs show that the physical appearance and stratigraphy of snow slabs is similar suggesting the possibility that they form a geometrical self-similar set of objects but, mathematically, the distribution of D does not display scale invariance over any significant range for the data in this paper.

[69] *Bak* [1996, p.63] suggested that it is difficult to estimate the noninteger (or fractal) power laws theoretically for self-similar criticality in a simple manner. This may be due partly to a lack of fundamental understanding of critical physical phenomena, the scaling issues involved and a corresponding lack of field data. The physical interpretation of the scaling law in relation to fracture in this paper is a combination of fundamental physics combined empirically with field data. The empirical form of the analysis presented here conforms with Bak's suggestion.

[70] Loose snow avalanches occur in cohesionless snow near the surface and, as such, they are somewhat analogous to the sandpile avalanches first analyzed by *Bak et al.* [1988]. Field observations show that, at a given time in an area, when loose snow avalanches occur they are all of approximately the same size. The size limitation is imposed by the depth of cohesionless snow at the surface. Once they start, they can sweep out the loose surface snow in combination with inertial effects. Below the surface, bonding and creep processes act to produce snow with cohesion which is not normally removed by small surface slides. Therefore it seems possible that loose snow avalanches may also have a fundamental length scale (depth of loose surface snow) which limits their size. The combination of inertial effects and a length scale suggests that analogous to sandpile avalanches, SOC as originally defined by *Bak et al.* [1987, 1988] will not directly apply to loose snow avalanches. It appears likely, then, that avalanches in nature (snow slab avalanches, loose snow avalanches, sandpile avalanches) do not conform to the original description of SOC. Since avalanches have been used as prototype examples to illustrate SOC, the definition of criticality and the system it is applied to may have to be carefully constructed to apply related concepts to events observed in nature.

[71] **Acknowledgments.** The research for this paper was supported by Canadian Mountain Holidays, the Natural Sciences and Engineering Research Council of Canada and the Vice President, Research, University of British Columbia. Data were provided by Juerg Schweizer and Canadian Mountain Holidays. I am grateful for all these sources of support.

References

Bak, P., *How Nature Works*, 212 pp., Springer-Verlag, New York, 1996.

Bak, P., C. Tang, and K. Wiesenfield, Self-organized criticality: An explanation of 1/f noise, *Phys. Rev. Lett.*, *59*, 381–384, 1987.

Bak, P., C. Tang, and K. Wiesenfield, Self-organized criticality, *Phys. Rev. A*, *38*, 364–374, 1988.

Bažant, Z. P., and J. Planas, *Fracture and Size Effect in Concrete and Other Quasi-brittle Materials*, 616 pp., CRC Press, New York, 1998.

Bažant, Z. P., G. Zi, and D. McClung, Size effect law and fracture mechanics of the triggering of dry snow slab avalanches, *J. Geophys. Res.*, *108*(B2), 2119, doi:1029/2002JB001884, 2003.

Bolt, B., W. L. Horn, G. A. Macdonald, and R. F. Scott, *Geological Hazards*, 328 pp., Springer-Verlag, New York, 1975.

Broek, D., *Elementary Engineering Fracture Mechanics*, 4th rev. ed., 516 pp., Kluwer Acad., Norwell, Mass., 1986.

Faillettaz, J., D. Daudon, and F. Louchet, Snow toughness measurements and possible applications to avalanche triggering, paper presented at International Snow Science Workshop, Int. Snow Sci. Workshop Can., Inc., Penticton, B. C., 29 Sept. to 4 Oct. 2002a.

Faillettaz, J., D. Daudon, F. Louchet, and J. R. Grasso, Scale invariance of snow triggering mechanisms, paper presented at International Snow Science Workshop, Int. Snow Sci. Workshop Can., Inc., Penticton, B. C., 29 Sept. to 4 Oct. 2002b.

Griffith, A. A., The phenomena of rupture and flow in solids, *Philos. Trans. R. Soc. London, Ser. A*, *221*, 163–197, 1921.

Griffith, A. A., The theory of rupture, in *Proceedings of First International Conference in Applied Mechanics*, pp. 55–63, J. Waltman Jr., Delft, Holland, 1924.

Hovius, N., P. A. Allen, and C. P. Stark, Sediment flux from a mountain belt derived by landslide mapping, *Geology*, *25*(3), 231–234, 1997.

Jamieson, J. B., Avalanche prediction for persistent snow slabs, Ph.D. thesis, 258 pp., Dep. of Civ. Eng., Univ. of Calgary, Calgary, Alberta, 1995.

Jensen, H. J., *Self-Organized Criticality*, 153 pp., Cambridge Univ. Press, New York, 1998.

Kirchner, H. O. K., G. Michot, and J. Schweizer, Fracture toughness of snow in tension and shear, *Scr. Mater.*, *46*, 425–429, 2002a.

Kirchner, H. O. K., G. Michot, and J. Schweizer, Fracture toughness of snow in shear under friction, *Phys. Rev. E*, *66*, 027103-1 to 027103-3, 2002b.

McClung, D. M., Direct simple shear tests on snow and their relation to slab avalanche formation, *J. Glaciol.*, *19*(81), 101–109, 1977.

McClung, D. M., Shear fracture precipitated by strain-softening as a mechanism of dry slab avalanche release, *J. Geophys. Res.*, *84*(B7), 3519–3526, 1979.

McClung, D. M., Fracture mechanical models of dry slab avalanche release, *J. Geophys. Res.*, *86*(B11), 10,783–10,790, 1981.

McClung, D. M., Mechanics of snow slab failure from a geotechnical perspective, in *Avalanche Formation, Movement and Effects*, *IASH Publ.*, *162*, 475–505, 1987.

McClung, D. M., The effects of temperature on fracture in dry slab avalanche release, *J. Geophys. Res.*, *101*(B10), 21,907–21,920, 1996.

McClung, D., and P. Schaerer, *The Avalanche Handbook*, 271 pp., Mountaineers, Seattle, Wash., 1993.

McClung, D. M., and J. Schweizer, Skier triggering, snow temperatures and the stability index for dry-slab avalanche initiation, *J. Glaciol.*, *45*(150), 190–200, 1999.

Mellor, M., A review of basic snow mechanics, *IASH Publ.*, *114*, 251–291, 1975.

Palmer, A. C., and J. R. Rice, The growth of slip surfaces in the progressive failure of over-consolidated clay, *Proc. R. Soc. London, Ser. A*, *332*, 527–548, 1973.

Perla, R., The slab avalanche, Ph.D. thesis, 100 pp., Univ. of Utah, Salt Lake City, 1971.

Perla, R., Slab avalanche measurements, *Can. Geotech. J.*, *14*(2), 206–213, 1976.

Roch, A., Les déchlencements d'avalanches, *IASH-AISH Publ*, *69*, 182–195, 1966.

Rosenthal, W., and K. Elder, Evidence of chaos in slab avalanches, paper presented at International Snow Science Workshop, Int. Snow Sci. Workshop Can., Inc., Penticton, B. C., 29 Sept. to 4 Oct. 2002.

Schweizer, J., Laboratory experiments on shear failure of snow, *Ann. Glaciol.*, *26*, 97–102, 1998.

Sinha, N. K., Constant stress rate deformation modulus of ice, paper presented at Sixth International Conference on Port and Ocean Engineering Under Arctic Conditions, Quebec City, 1981.

Sinha, N. K., Intercrystalline cracking, grain-boundary sliding and delayed elasticity at high temperature, *J. Mater. Sci.*, *19*, 359–376, 1984.

Stethem, C. J., and R. Perla, Snow-slab studies at Whistler Mountain, British Columbia, Canada, *J. Glaciol.*, *26*(94), 85–91, 1980.

D. M. McClung, Department of Geography, University of British Columbia, 1984 West Mall, Vancouver, British Columbia, Canada V6T 1Z2. (mcclung@geog.ubc.ca)